



ORIGINAL ARTICLE

Improvement of interfacial adhesion performance of the kevlar fiber mat by depositing SiC/TiO₂/Al₂O₃/graphene nanoparticles



Mohammad Asaduzzaman Chowdhury^a, Nayem Hossain^b,
Md. Bengir Ahmed Shuvho^c, Md. Arefin Kowser^d, Md. Akibul Islam^e,
Md. Ramjan Ali^f, Yaser A. EI-Badry^g, Zeinhom M. EI-Bahy^h

^a Department of Mechanical Engineering, Dhaka University of Engineering and Technology (DUET), Gazipur, Gazipur 1707, Bangladesh

^b Department of Mechanical Engineering, IUBAT-International University of Business Agriculture and Technology, Bangladesh

^c Department of Industrial and Production Engineering, National Institute of Textile Engineering and Research (NITER), Savar, Dhaka 1350, Bangladesh

^d Department of Mechanical Engineering, & Head of Department of Materials and Metallurgical Engineering, Dhaka University of Engineering and Technology (DUET), Gazipur, Gazipur 1707, Bangladesh

^e Department of Mechanical Engineering, Dhaka University of Engineering and Technology (DUET), Gazipur, Gazipur 1707, Bangladesh

^f Department of Mechanical Engineering, Dhaka University of Engineering and Technology (DUET), Gazipur, Gazipur 1707, Bangladesh

^g Chemistry Department, Faculty of Science, Taif University, Khurma, P.O. Box 11099, Taif 21944, Saudi Arabian

^h Department of Chemistry, Faculty of Science, Al-Azhar University, Nasr City 11884, Cairo, Egypt

Received 11 July 2021; accepted 24 August 2021

Available online 1 September 2021

KEYWORDS

Kevlar fiber;
Deposition;

Abstract Modern world seeks dramatic progress in composite materials use in numerous applications. Scientists worldwide are researching on fabricating new composites and attempting to have more applications using these materials. Serious attempts have also been taken to improve the properties of these materials. In this circumstance, a conscious attempt has been made in this present

E-mail addresses: asad@duet.ac.bd (M.A. Chowdhury), nayem.hossain@iubat.edu (N. Hossain), bengir.duet@gmail.com (Md. Bengir Ahmed Shuvho), arefin@duet.ac.bd (M.A. Kowser), ramjan@duet.ac.bd (M.R. Ali), Y.elbadry@tu.edu.sa (Y.A. EI-Badry), zeinelbahy@azhar.edu.eg (Z.M. EI-Bahy)

Peer review under responsibility of King Saud University.



Production and hosting by Elsevier

Adhesion;
SiC;
Graphene;
TiO₂

work that studies the effect of SiC/TiO₂/Al₂O₃/ graphene nanoparticles (NPs) deposition on Kevlar fiber. In this process, SiC/TiO₂/Al₂O₃/ graphene NPs have been deposited on Kevlar fiber by dip coating process. For the analysis, physical observation has been performed well at first which confirms nanoparticle deposition on the fiber and formation of adhesive bonding. SEM analysis followed by surface topography has been conducted to observe and further analysis of nanoparticle deposition. Atomic bonding mechanism shows how chemical bonding between fiber and nanoparticles. TGA analysis shows thermal improvement of the fiber by NPs deposition where graphene with binder makes 21.6% improvement in decomposition temperature. Tensile strength and young's modulus of binder inclusion coated kevlar fabric are improved up to 26% and 5.7%, respectively. Finally, the IR-spectra confirms successful deposition of nanoparticles on the fiber.

© 2021 The Author(s). Published by Elsevier B.V. on behalf of King Saud University. This is an open access article under the CC BY license (<http://creativecommons.org/licenses/by/4.0/>).

1. Introduction

Kevlar is a thoroughly aromatic polyamides and it is an extensively used fiber reinforced materials in aerospace, spacecraft, automobile, and military applications because of its high specific strength, high elastic modulus, lightweight, low density, high resistance to abrasion, and chemical stability as a synthetic fiber (Chakraborty et al., 2020; Reuben et al., 2020; Sreejith and Rajeev, 2021). Kevlar is a widely used in composites as fiber bundles, continuous filaments, pulp, short cut fibers, fabric, paper and powder based on application. However, Kevlar is a chemically inert, highly crystalline structure and smooth surface which drive to poor interface with the matrix due to its chemical structure. The chemical structure of Kevlar keeps down its use owing to difficulties of matrix adhesion. Adhesion is crucial in composite material applications because it effects the durability and functionality of structure of the composites. Due to this reason, surface treatment techniques such as ultrasonic treatment, γ -ray irradiation, plasma treatment, etching, cryogenic treatment and chemical grafting are used to resolve the issues and to improve interfacial adhesion strength (Yang et al., 2019; Lu et al., 2018; Bulut et al., 2018). These techniques can be classified into two categories chemical and physical type. The chemical type surface treatment techniques have considerable effects of modification on the fiber surface. However, these techniques are hard to control, complex, damage the surface properties of the fiber (Li et al., 2019). In contrary, physical type surface treatment techniques are easy to control, simple, but may result in poor strong interfacial adhesion than chemical treatment techniques. In addition, chemical and physical type surface modification techniques are multi-step procedure, limited with strict reaction and high-cost instrument.

Coating is a significant fiber surface treatment or modification technique which provided potential enhancement of the surface interface. Moreover, this technique can retain the main surface structure, resolve defects of surface of the fibers and it is compatible for complex shape samples. Recently, thin film deposition using NPs onto surface of the fiber has been identified to be an efficient surface treatment technique as the NPs make more corrugated surface of the fibers and accordingly improve the fertilization capability between the fiber and the polymer matrix. In addition, the reactive group of the NPs that may contain in the NPs may yield chemical bonding interaction to ameliorate the interfacial adhesion between the fiber surface and polymer matrix. Reuben et al. (Chakraborty et al., 2020) studied biometric surface treatment method for aramid fiber to improve the interface properties between the epoxy resin and modified aramid fibers. The graphene oxide (GO) was utilized to graft on the surface poly dopamine coated aramid fibers. They found surface modification enhanced the interfacial shear strength by 210%.

Li et al. (2019) conducted Kevlar fiber surface treatment deposited with nano SiO₂ and they found that the strongest adhesion and shear strength between the Kevlar fiber and the epoxy resin and improved

the shear strength 83.6% higher than original composites. Haijuan et al. (2019) investigated Kevlar fiber surface modification with supercritical carbon dioxide (ScCO₂) with acetic anhydride to enhance the mechanical properties and the interfacial adhesion. They increased the shear strength and tensile strength of the composites 47.9% and 21.3% than untreated composites, respectively. Moreover, they found that the ScCO₂ treatment technique is safe for environment for surface modification to enhance the interfacial bonding between treated Kevlar fiber and the matrix. Patterson and Sodano (2016) characterized surface modification of the aramid fibers with ZnO NPs deposition that concurrently improved UV absorption and interfacial adhesion of the fiber reinforced composites. They found the surface modification with ZnO NPs deposition improved the interfacial shear strength 18.9% of the treated aramid fibers than those of untreated Kevlar fibers. Bulut et al. (Sharma et al., 2019) conducted a comprehensive study to enhance the interfacial bonding between carbon/Kevlar/epoxy deposition with nano silica. The modified fiber reinforced composites showed that the flexural strength and tensile strength improved by 35.7% and 20% respectively.

In literature (Wen et al., 2020; Wen et al., 2019; Bi et al., 2020; Xie et al., 2020), the fiber mat attributed to nanoparticles are investigated to change the requisite properties. The thermal conductivity of TiO₂-Al₂O₃ aerogel-SiO₂ fiber mat composite is reduced by doping first rutile-typed TiO₂ and then after heated with temperature doping by SiC (Wen et al., 2020). Al₂O₃ aerogels and Al₂O₃ aerogel-SiO₂ fiber composite is made by sol-gel method for improving thermal insulation for high heat resistance (Wen et al., 2019). The uniformity, elasticity and hydrophobicity of methyltrimethoxysilane (MTMS)-based silica aerogels were prepared which have failure strain as much as 66.14%. Due to superior properties of MTMS based silica aerogel, such as lightweight, superhydrophobic and flexibility, it is promising for defense, civil and building construction applications (Bi et al., 2020). The Nitrogen-doped porous Graphene-based aerogels including different chitosan elements were fabricated by the hydrothermal reaction. The density of graphene-based aerogels reduces and their specific surface area increase slowly with the increase of chitosan element (Xie et al., 2020). These concepts of nanoparticles related aerogel can be extended by attributing it with the fiber mats for their multifunctional application in industry.

In general, different methods are used to improve the interfacial adhesion between the different fiber mats and deposited nanoparticles for confirming the better thermal and mechanical properties. Beside this, to understand the role of nanoparticles for improving the other properties as a deposited material can be investigated in future. As for example, CNT (carbon nanotube) and gold have the property of increase the photocatalytic efficiency of TiO₂ and TiO₂-SiO₂. In case of CNT/TiO₂ and Au/TiO₂ composites, CNT and Au are used as electron receptors to improve the photo-activity of TiO₂ (Chinh et al., 2019). The CNT/TiO₂-SiO₂ composite in comparison of Au-CNT/

TiO₂-SiO₂ addressed the higher photocatalytic behavior toward the degradation of methylene blue. Using different strategies, enhancing the photocatalytic activity of graphene nanoparticle as graphene composite, water purification is done (Singh et al., 2020). Al₂O₃-GO nanoparticle-based carbon paste electrode is considered as potential electrode for NADH (dihyronicotinamide adenine dinucleotide) level detection in enzymatic applicability in practice (Mekawy et al., 2018). Apart from this, bio-based nanoparticles are used for biomedical to different range of applications (Wang et al., 2021; Anwar et al., 2021; Shoaib et al., 2021; Nazir et al., 2021; Arriaza-Echanes et al., 2021; Farias et al., 2021; Dara et al., 2021; Chen et al., 2021; My-Thao Nguyen et al., 2021).

From the discussion of the literatures, it is identified that Kevlar fiber mat deposition with SiC, TiO₂, Al₂O₃, Graphene NPs was not conducted yet to improve the interfacial adhesion of the Kevlar fibers. The structure, morphology and properties of the both Kevlar fiber mat and NPs modified were investigated. This characterization study was aimed at demonstrating that the NPs deposition interface can improve the interfacial adhesion performance of the Kevlar fiber mat.

The novelty of this study is to use Kevlar fabric or mat that has not been used previously by coating different type of nanoparticle on it under with and without binder addition. The thermal and mechanical properties of Kevlar mat are increased noticeably after coating with nanoparticles by the improvement of interfacial adhesion performance. The coated Kevlar mat can be used as reinforcing phase for the fabrication of composite materials to improve their physical properties for extending their applications in different areas. It can be expected that coated Kevlar reinforced composites will exhibit higher physical properties than that of the Kevlar composites when coatings are absent. The suitable selection of nanoparticles and their coatings on Kevlar mat can be attributed to the advancement of knowledge in energy storage process, semiconductor applications, automotive applications, aerospace technology, insulator fabrication, fuel cell, biomedical sensors, supercapacitors, waste water treatment, food industries, corrosion resistance and the applications where the high temperature and superior mechanical properties are important.

2. Methodology

2.1. Materials

In present study commercially available Kevlar fiber mats (1.5 mm thickness) were purchased from Richest Group Ltd of China. In general, Kevlar fiber mats are used as a reinforcing phase to improve the qualities of the composite materials. To enhance the applicability of this mat, Al₂O₃, Graphene, SiC and TiO₂ nanoparticles are used to deposit on the surfaces of Kevlar mat. The nanoparticles are purchased from Shanghai Ruizheng Chemical Technology Co., Ltd of China. The qualities of Al₂O₃ NPs (Model: AIN-001, average particle size: 30 Nm, purity = > 99.9%, specific surface area = 42 m²/g, density = 0.15 g/cm³, shape = hexagon, color = white), SiC (Model: SiC-001, average particle size: 40 Nm, purity = > 99.9%, specific surface area = 39.8 m²/g, density = 0.11 g/cm³, shape = cube, color = grey green), graphene (purity = > 95 wt%, thickness = 3.4–7 nm, diameter = 50 * 50 μm, electrical conductivity = 10⁵ sm, Oxygen content: 0.5%, Sulphur content: 0.5%, layers = 6–10, SSA: 100–300 m²/g, appearance: black) and TiO₂ (particle size: 10 nm (R), purity: 99.5%) were provided by the materials supplier. Polyvinyl alcohol (1.19–1.31 g/cm³) was used as a binder substance which purchased from the local market. PVA is a water soluble synthetic polymer having the chemical formula [CH₂CH(OH)]_n. It has high tensile strength and flexibility,

high oxygen and aroma barrier properties and film-forming, emulsifying and adhesive properties.

Kevlar fibers are aromatic polyamide threads which is combined by para-phenylenediamine and terephthaloyl chloride. The yellow color of the Kevlar fiber (KF) is produced by the combination of strong and weak electron system bonds in different directions of polymer chains. When fibers are bended in a loop, they become twisted internally resulting its properties into the composites. Existing interchain bonds, molecular hydrogen bonds make kevlar highly resistive. Spun kevlar shows high tensile resistance as well due to the formation of intermolecular hydrogen bonds between carbonyl groups and nitrogen–hydrogen bonds. Relatively rigid molecules form kevlar structure resulting sheet like structure. Kevlar fiber is mainly used in textiles as composites (Zhu et al., 2011; Saba and Jawaid, 2017; Kowsari et al., 2019). The morphology of Kevlar mat in Fig. 1 shows the plain weave fabric with clean and smooth surfaces (Zeng et al., 2018; de Oliveira Braga et al., 2018). Fiber weaving process in different directions and Kevlar fibers are clearly appeared. The morphology of nanoparticles is illustrated in Fig. 2.

The exponential distribution for grain size of aluminium oxide nanoparticles is observed from the figure. High quality quantum dots are appeared. SEM image indicates that the distribution of nanoparticles is non-uniform throughout the entire surface. Some agglomeration of the nanoparticles is also formed. This is due to the interfacial surface tension and appearance of the quantum dots (Bodke et al., 2015; Jbara et al., 2017).

In this figure, SiC and TiC nanoparticles are seen as a cube or spherical, non-uniform and irregular shape particles. The agglomerated and rounded particles are also observed (Mahawish et al., 2017). In this case, agglomeration of particles is supposed to relate with the Van-der Waal forces that act between the individual particles. Moreover, chainlike aggregated nanostructures are evident for SiC nanoparticle (Rajarao et al., 2014). The smooth surface morphology of graphene is observed in which nano-scale platelet structure is clearly formed (Ren et al., 2020).

2.2. Dip coating process

Solution dip-coating technique is utilized for thin film deposition on Kevlar fibers because of it is the simplest technique and is usually exploited in scale up coating fabrication. Kevlar fabrics (10 cm × 10 cm) were cut and used for the pulling technique which were immersed with the nanoparticle solutions (Fig. 4). The samples were perpendicularly pulled into the solution. The samples are let to immersed into the solution to allow some time for nanoparticle deposition. After this, the samples are withdrawn out from the solution and let to dry. The process can be divided into three steps namely immersion and immersion time, deposition and drainage, and solvent evaporation. In immersion and immersion time, Immersion of the substrate is typically done perpendicularly although a different type of angled immersion has also been tested for asymmetrical deposition thicknesses. The immersion is controlled by a computer for automated dipping and constant dipping speed. After immersion, the substrate is kept in the solution to allow enough time for complete wetting of the substrate. The solutions were prepared with 2% of nano-particles. Here, the func-

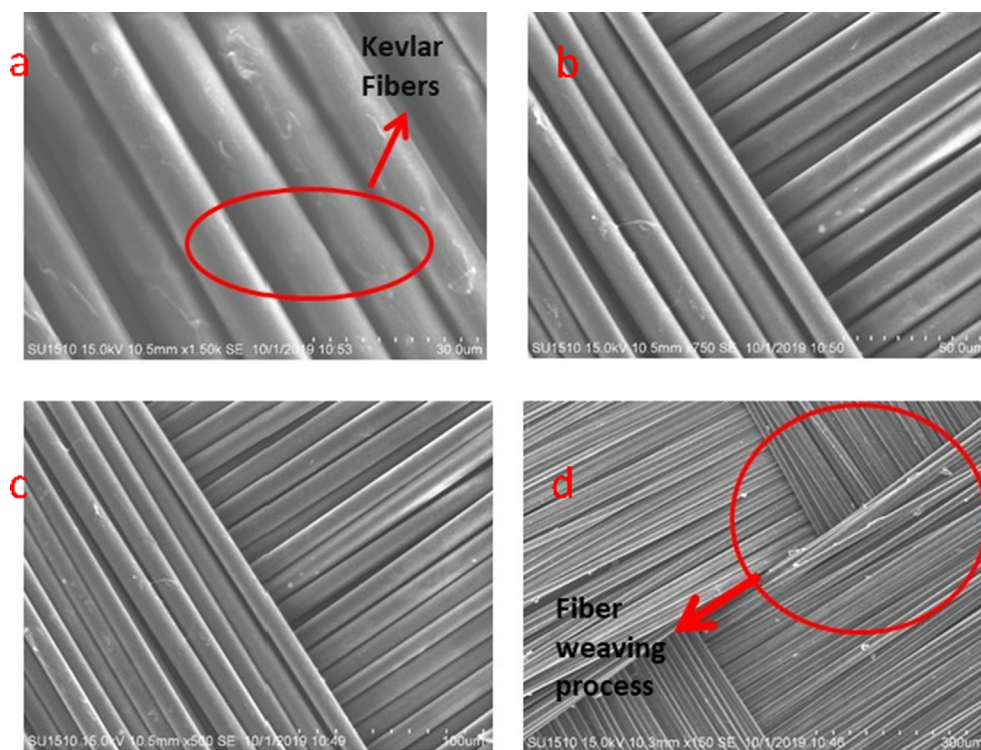


Fig. 1 SEM morphology of Kevlar fiber at (a) 3.3x, (b) 10x, (c) 20x and (d) 33.3x magnification.

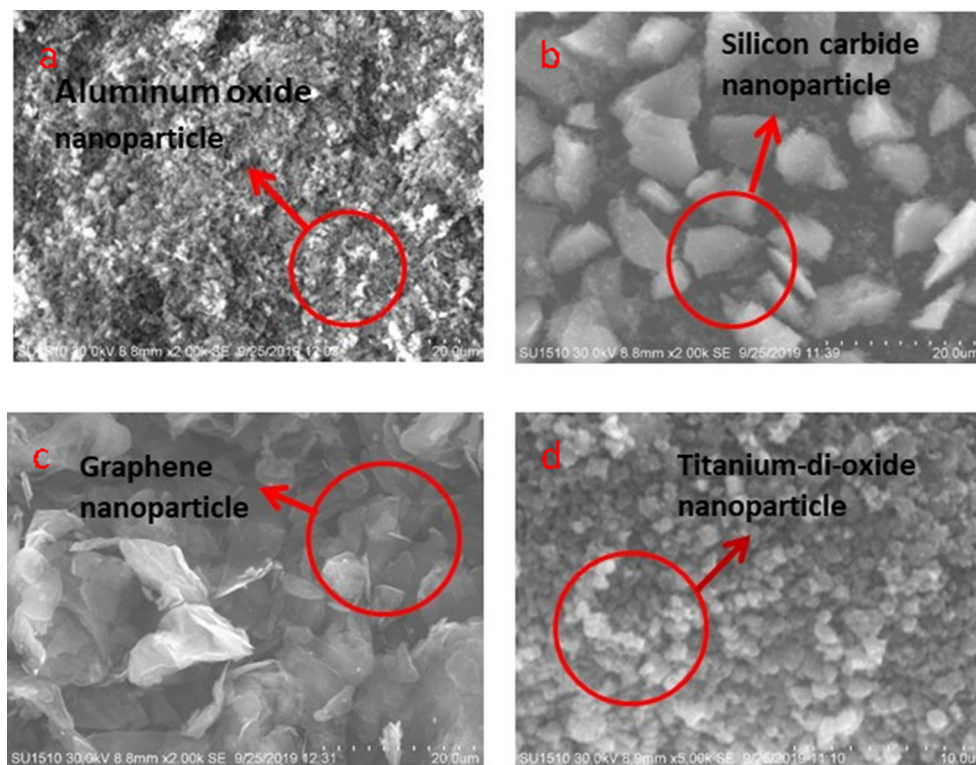


Fig. 2 SEM morphology of (a) aluminum oxide at 50x, (b) silicon carbide at 50x, (c) graphene at 50x and (d) titanium-di-oxide at 100x magnification.

tionality of the both, initial substrate surface and the nanoparticle surface, plays an important role. After the immersion

time, the substrate is pulled out from the solution at pulling rate of $100 \mu\text{m/s}$ from the 2% nano particles solution. The

speed at which the substrate is pulled is meaningful. Higher withdrawal speed leads to thicker coatings. The speed should be thus kept constant the whole length of the substrate and any undesired vibrations should be avoided. The concentration of the solution is also an important parameter. Too low concentration will lead to an uneven coating of the substrate. High concentration solution tends to cause aggregation of nanoparticles already in the solution phase leading to multi-layered assembly of nanoparticles. Evaporation stage is for the solvent to evaporate from the produced film. Here, the samples are dried at 75 °C for 1 h in a dry oven. The evaporation time depends on the solvent used and can be promoted by heating of the substrate. If very volatile solvents are used, such as alcohols, the evaporation will start already at the drainage stage. A laboratory padding mangle was used to squeeze out the excess water from the Coated Kevlar fiber at a pressure 1 kg/cm². The full experimentation is shown in Fig. 3.

2.3. Procedure of decomposition temperature determination

Thermal Gravimetric Analyzer (Model: SDT 650 Simultaneous Thermal Analyzer, Serial no.: 0650-0180, Sample Interval: 0.1 s/pt, Ramp Segment 10 °C/min to 1400 °C Started, Pan type: Alumina 90 µl) is used to determine thermal decomposition temperature of coated sample by oxidation or reduction in which the mass of the coated sample is measured over the time as the temperature changes. A data acquisition system is used to collect the data of temperature vs weight loss and heat flow continuously when the system is on and these data are sent directly to the computer. The graph is also plotted automatically by the computer programming. From the graph of temperature vs weight loss, the point where the coated fiber material starts disintegrating is identified as an initial decomposition temperature. The maximum rate of decomposition temperature is evaluated in the regime where the maximum amount of coated fiber material is decomposed. Beside thermal decomposition, the other parameters such as, absorption, desorption, and phase transition are also analyzed. For this

work, a heating rate of 100 C/min was provided up to 1000 °C in a nitrogen environment. The thermal gravimetric analyzer (TGA) set up used for measuring decomposition temperature is illustrated in Fig. 4.

3. Results and discussions

3.1. Physical analysis of coated Kevlar mat

Fig. 5(a) represents the optical image of Kevlar used in this study. Two phenolic rings are connected in Kevlar monomer chain with the help of one para-amide in axial direction and hydrogen bonds connect these monomer chains radially which makes their fibers highly crystal when extruded (Sharma et al., 2019). The presence of Al₂O₃ NPs on Kevlar fiber mat is seen in Fig. 5(b). The color of the surface of Kevlar fiber has been changed due to the presence of Al₂O₃ NPs. Fig. 5(c) represents the Al₂O₃ NPs with binder on Kevlar surface. Binder changed the color of the surface of Fig. 5(c) than Fig. 5(a). The presence of black color on Kevlar fiber proves the presence of graphene nanoparticles shown in Fig. 5(d). The presence of binder with graphene makes the surface darker which is seen in Fig. 5(e). Fig. 5(f) and Fig. 5(g) show the presence of SiC NPs and SiC NPs with binder. Fig. 5(h) and Fig. 5(i) show the presence of TiO₂ NPs and TiO₂ with binder. Binder differentiated the color of the surface from titanium di-oxide. In case of nanoparticles, without binder some particles are pushed into the internal surfaces of the Kevlar mat, some of the NPs are broken to adhere on the upper surfaces of the mat. Some other particles are diffused through the surfaces. All of these nanoparticles on Kevlar strengthen the surfaces. The angle and roughness of the NPs infused coating develop adequate surface tension to confirm that than soaking effects into it (Nahum et al., 2017). The mechanisms of formations of coating are observed to be different when NPs incorporates with binder. In case of binder addition, the NPs are melted and uniformly distributed throughout the mat surfaces, there is no any NPs that are pushing down into the nano-holes of the surfaces.

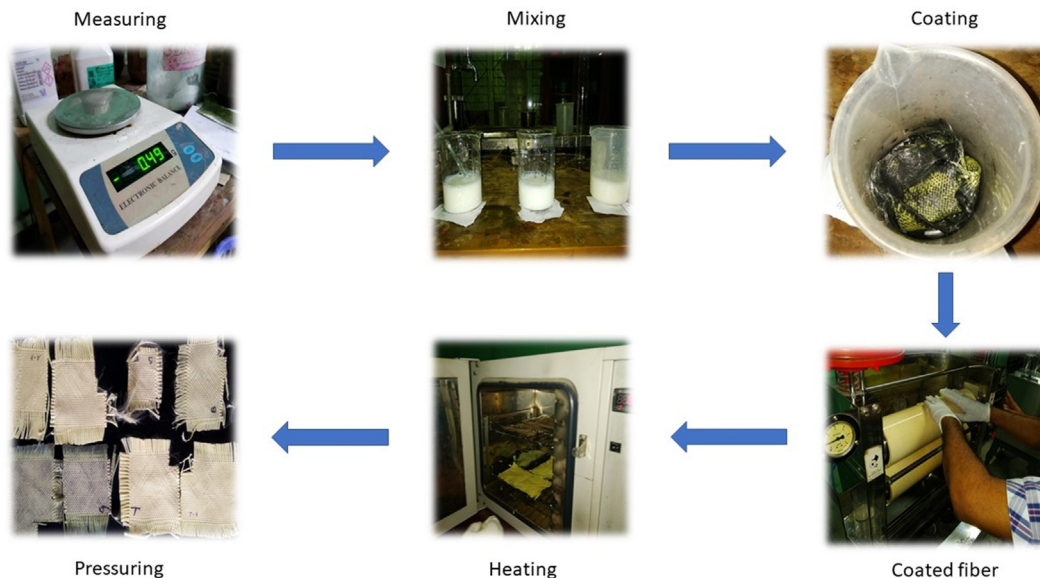


Fig. 3 Dip coating process.



Fig. 4 TGA setup for determination of decomposition temperature.

Due to the combined modes of nanoparticles on Kevlar surfaces, produce adhesive forces in the interface which results to cause enough energy dissipation within the interfacial layers adjacent to the fibers embedded. In physical observations, it is also evident that after surface modifications in both cases surfaces are seen to be rougher. But the surfaces with binder are smoother than that of the surfaces without binder. As the surface roughness is related to the tribological responses, the surfaces without binder can exhibit more friction than that of surfaces with binder (Zhou et al., 2015). The weight of the surfaces with binder are higher in comparison with the surfaces without binder. The binders squeeze the Kevlar mat in certain

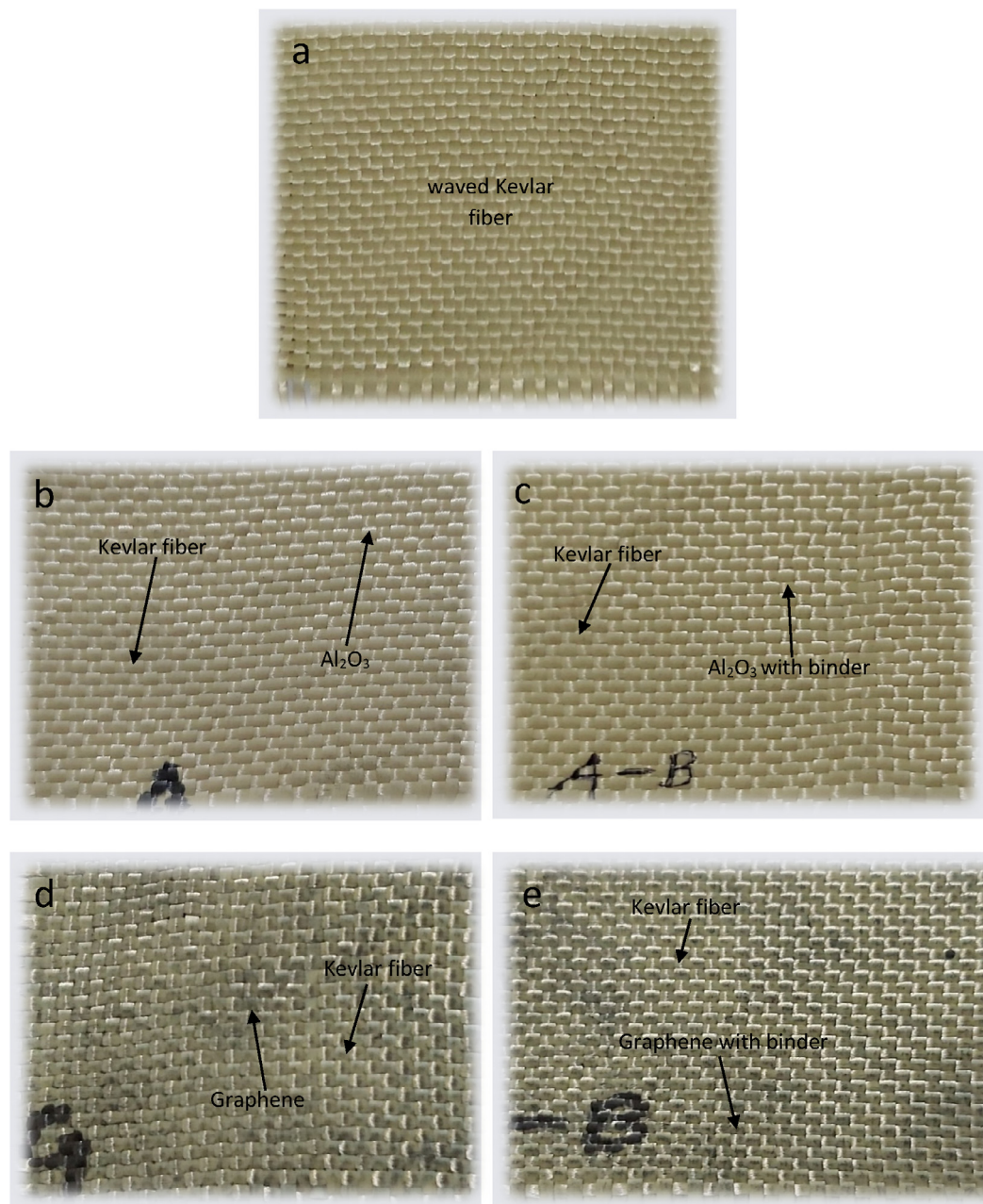


Fig. 5 Visual analysis of (a) Kevlar Fiber (Standard), (b) Al_2O_3 coated fiber, (c) Al_2O_3 coated fiber with binder, (d) Graphene coated fiber, (e) Graphene coated fiber with binder, (f) SiC coated fiber, (g) SiC coated fiber with binder, (h) TiO_2 coated fiber, (i) TiO_2 coated fiber with binder.

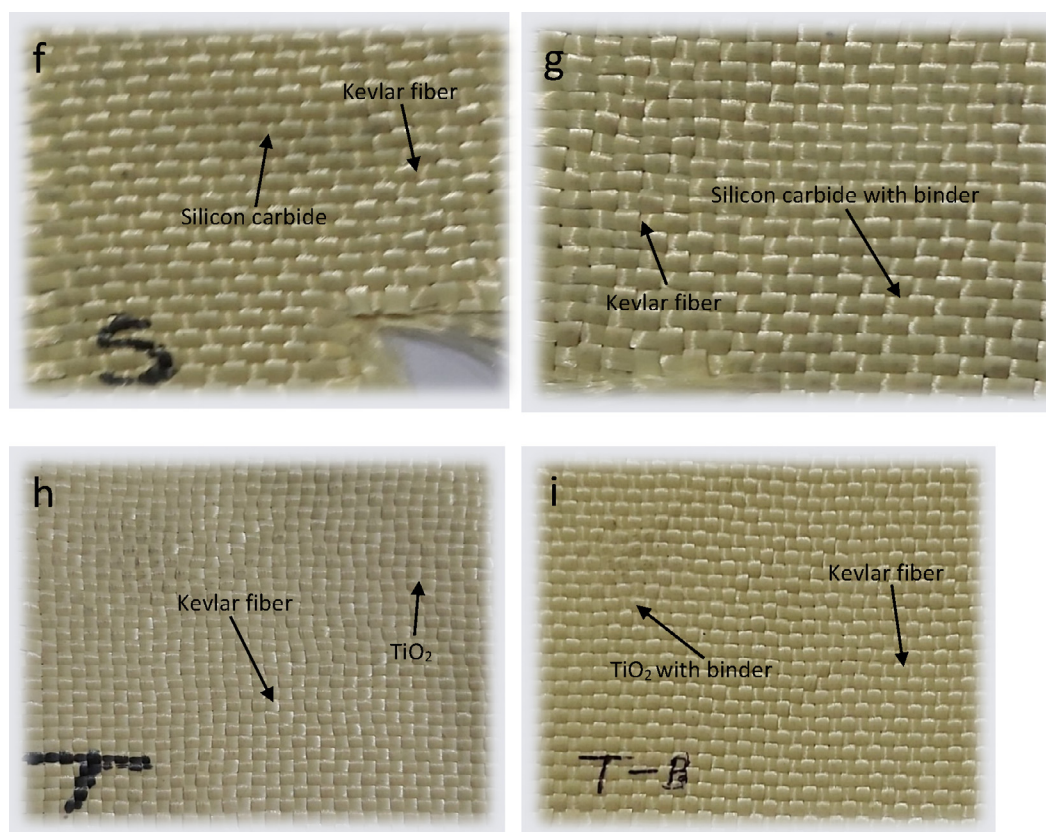


Fig. 5 (continued)

extent. However, in case of without binder, the mat is seen to be straight, flexible and more compact.

3.2. SEM characterization of coated Kevlar MAT

The most extensive used tool is SEM for surface analysis in materials science. Fig. 6 represent SEM images of NPs deposition or adhesion in Kevlar fiber mat. Fig. 6(a) represents pure Kevlar fiber mat and no NPs were added. This figure represents pure Kevlar fiber mat and no NPs were added. The surface is seen clean and smooth and the fibers are firmly spun with each other. Fig. 6(b), Fig. 6(c) show Al_2O_3 NPs coated fiber without and with binder. Dispersion of Al_2O_3 NPs is clearly visible as seen in Fig. 6(b) and almost homogenous. Similar phenomena are also observed for TiO_2 as seen in Fig. 6(h) and (i). However, in case of graphene NPs and SiC NPs, there are less visible of particles dispersion. From the SEM observation, Graphene NPs concentrated less due to small pores between the weft and warp threads (Mahbub et al., 2014). However, porosity and morphology depend on size of the graphene sheets (Wang et al., 2013). In addition, Al_2O_3 and TiO_2 NPs show higher adhesion into the Kevlar mat this is because of three-dimensional porous structure, surface tension force and capillary effect of the Kevlar fibrous mat (Ke and Li, 2018).

3.3. Surface topography

The particle dispersion through Kevlar mat by Al_2O_3 , SiC, TiO_2 and Graphene with and without binder is shown in

Fig. 8. The figure illustrates that the interfacial adhesion between NPs infused binding element and Kevlar mat surfaces are higher than that of the NPs depositing mat surfaces where the binder is absent. When only NPs is used as coating materials on the substrate surfaces, then agglomeration is occurred. Due to formation of agglomeration, the particles are adhered loosely with the substrate surfaces which can usually be broken by mechanical forces. This is associated with the reduction of effectiveness for obtaining improved adhesive properties of nanoparticles in the surfaces of fiber mat (Zare and Garmabi, 2012; Zare et al., 2011; Dorigato et al., 2013). The literature (Zare, 2016; Zare, 2016) have reported that any accumulation of nanoparticles (agglomeration) effects adversely the stiffness of embedded fibers, by decreasing the interfacial contacts between layer of coating and substrate. Moreover, some defects and stress concentrations are produced in interfacial surface of coating layer and Kevlar mat (Zare, 2016; Müller et al., 2014).

Homogeneous and compatible particle distribution and well dispersion is attributed in case of SiC and TiO_2 , thereby improving the strength of the material for formation of coating layers (Jana et al., 2013). However, dispersion of Al_2O_3 and graphene nanoparticles is not evident as well as SiC and TiO_2 nanoparticles in the surfaces of the substrate. Well compatibility and dispersion lead to address superior rheological, mechanical, water absorption, and thermal behavior (Cicco et al., 2017; Yang et al., 2020). Fig. 7(a) indicates that particle dispersion of Al_2O_3 including binder is more in comparison of Al_2O_3 when binder is not considered. In case of Al_2O_3 and binder mixture, the homogeneity is more visible in thin film coatings. Similar trends are also observed in case of SiC, TiO_2 and

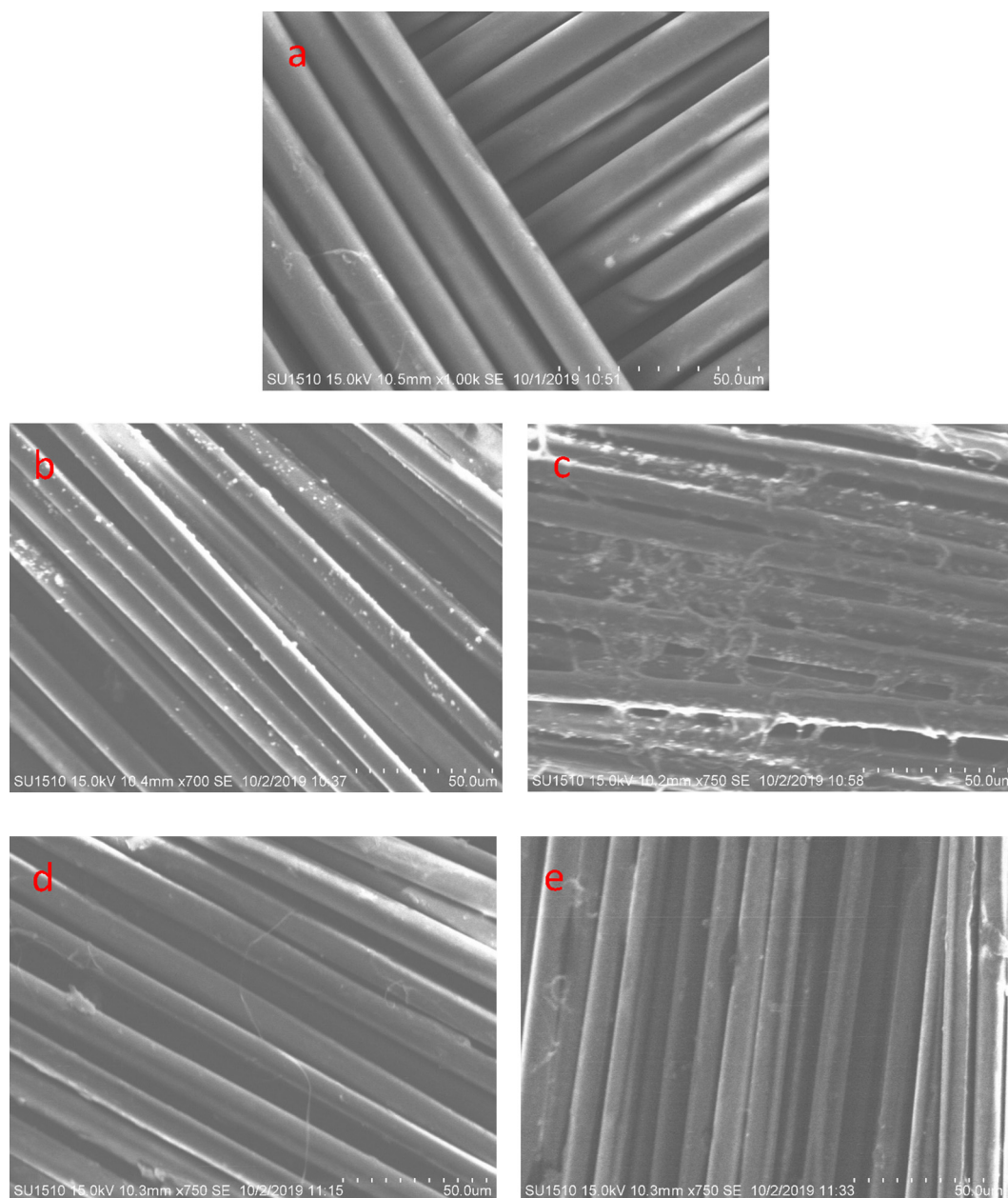


Fig. 6 SEM analysis of (a) Kevlar Fiber (Standard), (b) Al_2O_3 coated fiber, (c) Al_2O_3 coated fiber with binder, (d) Graphene coated fiber, (e) Graphene coated fiber with binder, (f) SiC coated fiber, (g) SiC coated fiber with binder, (h) TiO_2 coated fiber, (i) TiO_2 coated fiber with binder.

graphene as which are depicted in Fig. 7(b), (c) and (d). The characteristics of coating surface roughness or topography of the surfaces are clearly appeared on the Kevlar fiber mats. Fig. 8 confirms that the surface topography is smooth, when nanoparticles are mixing with binder solution for the formation of thin film on substrate surfaces. However, the coating surfaces without binder are exhibited the higher roughing property.

3.4. Atomic bonding mechanism

The Kevlar fibers have large molecular chains which are parallel to each other. Each Kevlar molecular chain is bonded by one to five million monomers (Cheng et al., 2005; Yang,

1993; Cao et al., 2013). The orientation of the molecules in fibers is described as a crystalline structure which causes anisotropy property. The structures of nanoparticles of materials in general are determined by the chemical composition of the materials, the number of atoms available in the particles and the character of the chemical interaction among atoms. Nanoparticle is comprised of a regular crystalline structure. This structure can be in the form of amorphous or a pseudo close packing which is indescribable by any of the crystallographic space groups. In case of each structural states of a nanoparticle, the certain set of number of atoms is associated with the particle that leads to optimal stable configurations (Shevchenko and Madison, 2002).

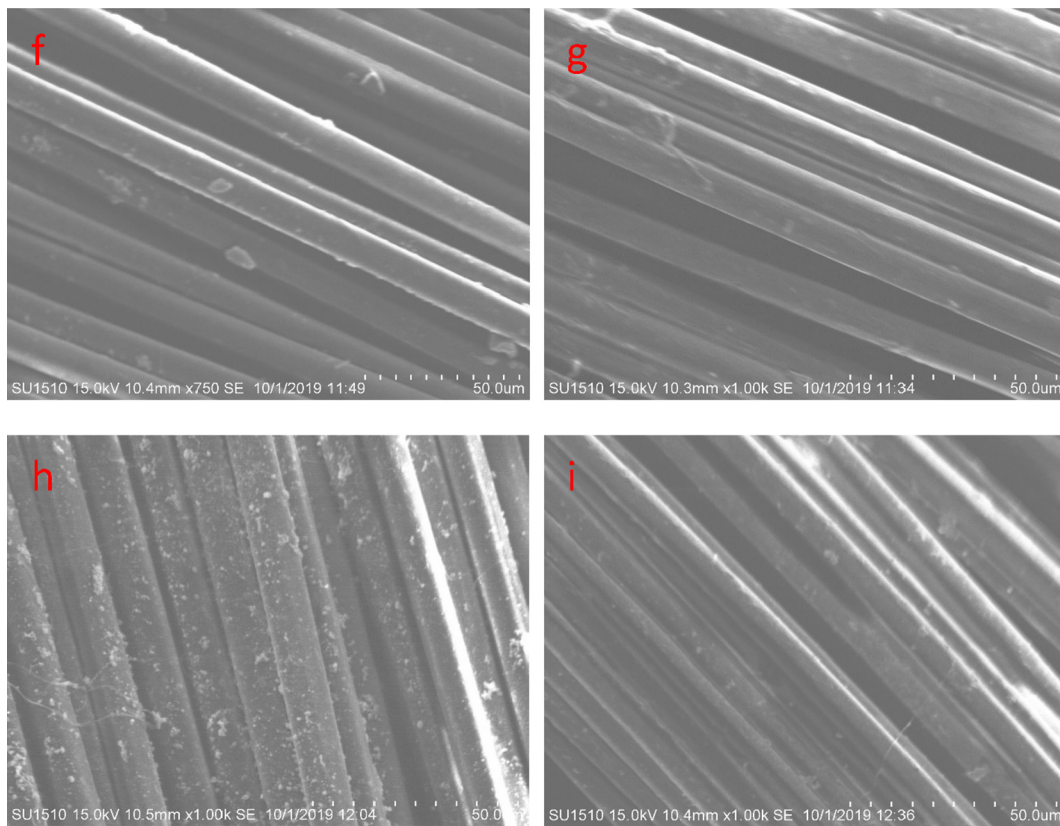


Fig. 6 (continued)

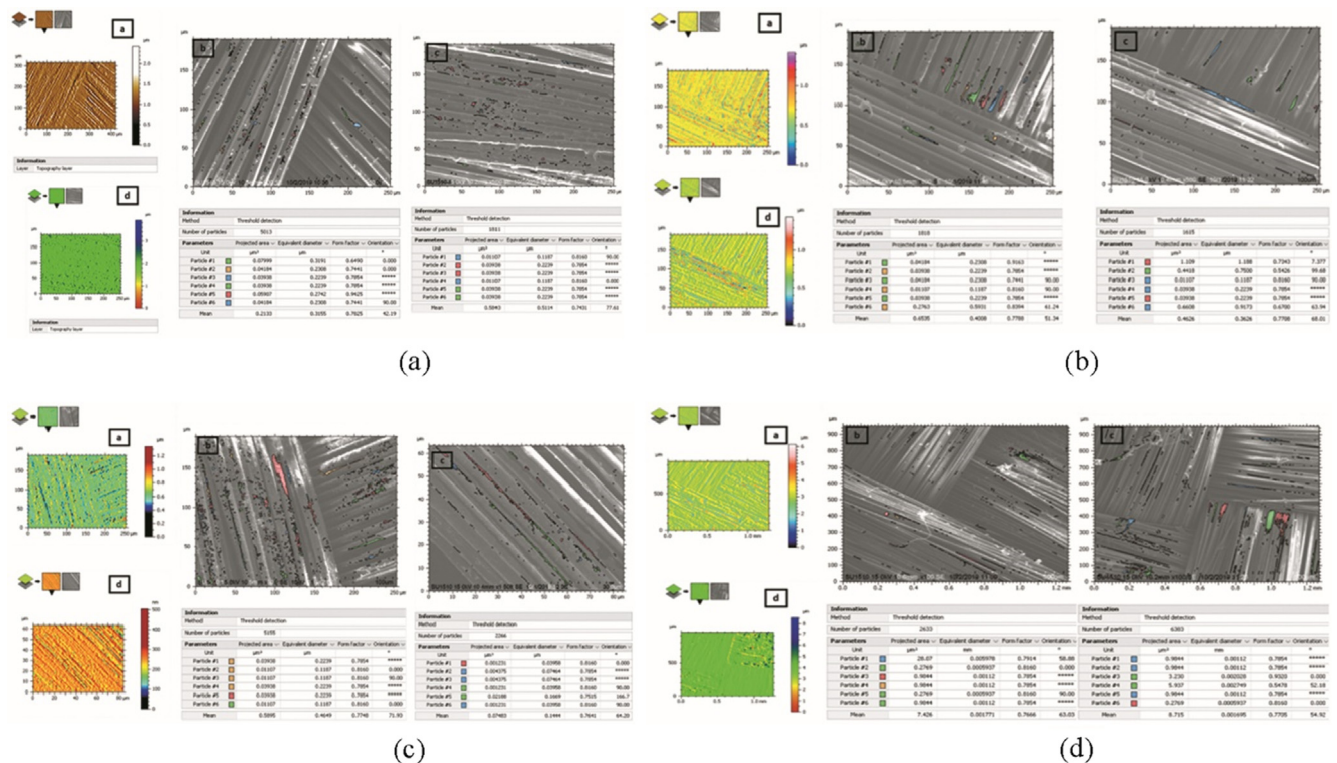


Fig. 7 Particle dispersion through on Kevlar mat by (a) Al₂O₃, (b) SiC, (c) TiO₂ and (d) Graphene with and without binder.

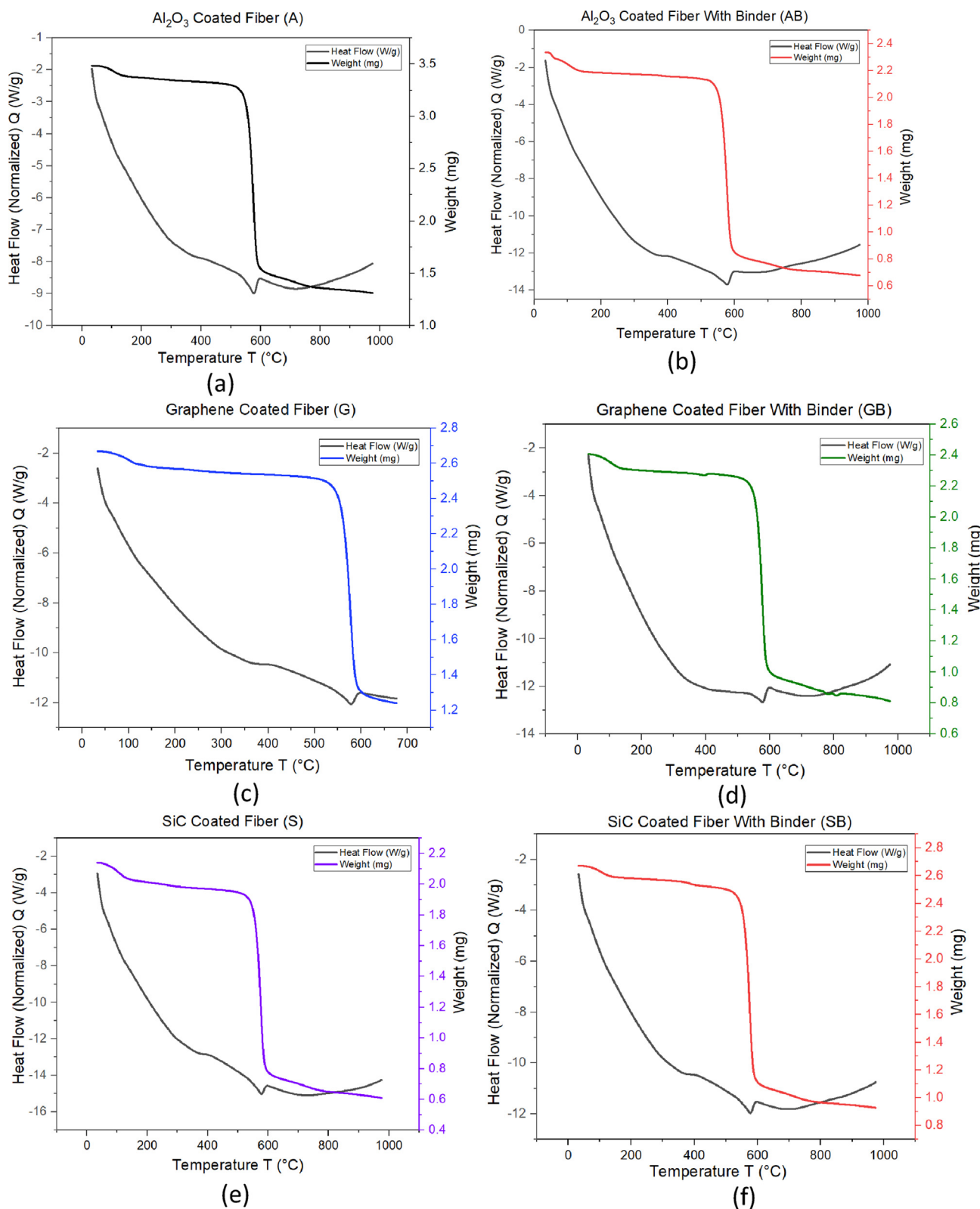


Fig. 8 TGA and DSC analysis of (a) Al_2O_3 coated fiber, (c) Al_2O_3 coated fiber with binder, (d) Graphene coated fiber, (e) Graphene coated fiber with binder, (f) SiC coated fiber, (g) SiC coated fiber with binder, (h) TiO_2 coated fiber, (i) TiO_2 coated fiber with binder.

During coating process, chemical bond is formed between nanoparticle and the surfaces of the Kevlar mat by the attachment of one atom or molecule with the other through the func-

tionalization process. Some molecules of adhesives in combination of nanoparticles chemically react with the molecules of Kevlar mat materials and become hardened, because

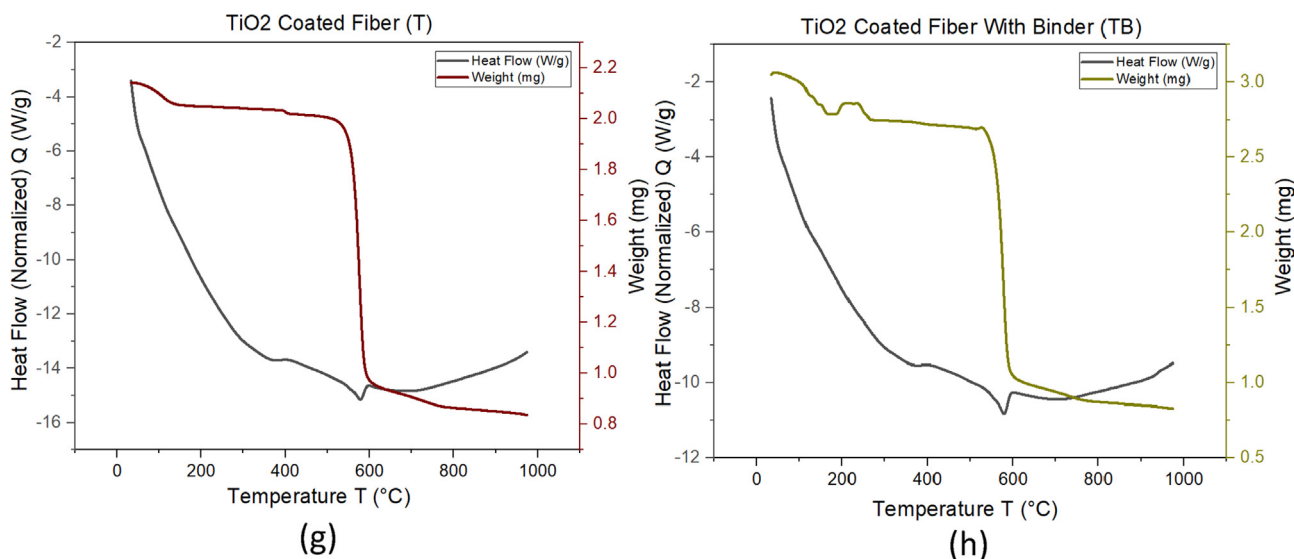


Fig. 8 (continued)

of this adherends are bond together (Pequegnat and Zhou, 2013). The formation of chemical bond changes the properties of the fibers of Kevlar mat.

Apart from chemical bond, during functionalization process, covalent or a van der Waals bond is formed within the interfacial layers. In covalent bond, one or more pairs of valence electrons are shared between the atoms through the adjacent layers of the substrate and nanoparticles which results in strong bond. In physical adsorption process, van der Waals forces exists between the molecules of adhesives in combination of nanoparticles and the molecules of fiber mat materials and bonds them together (Pequegnat and Zhou, 2013).

In a van der Waals bond, due to presence of electrostatic attraction, positively and negatively charged atoms is created a bond between the nanoparticles and the mat surfaces. The strength of this bond is less than that of covalent bond; however, it plays some roles to hold the coating materials on the surfaces of the fiber mat by the formation of bond. The bonding characteristics are different for different nanoparticles depending on their distinct properties. The bonding mechanism between the coating layers and the surface of the substrate is confirmed by the other research works available in the literature (Booker and Boysen, 2005; Tian et al., 2017).

3.5. Improvement of thermal property of coated Kevlar mat

Fig. 8 represents the TGA and DSC analysis of coated Kevlar mat. The decomposition temperature for standard Kevlar fiber in air is varied from 427 °C to 482 °C (Ioffe, 2010; Chaitap et al., 2009). In this study, the decomposition temperature of Kevlar fiber after coated with nanoparticles are measured around the range of 530 °C to 585 °C for Al₂O₃, 540 °C to 590 °C for Al₂O₃ with binder, 540 °C to 590 °C for graphene, 545 °C to 595 °C for graphene with binder, 540 °C to 585 °C for SiC, 545 °C to 590 °C for SiC with binder, 535 °C to 585 °C for TiO₂ and 540 °C to 590 °C for TiO₂ with binder. Considering the decomposition temperature (427 °C to 482 °C) of standard Kevlar fiber, the decomposed temperatures for Al₂O₃, graphene, SiC and TiO₂ nanoparticle depos-

ited Kevlar are enhanced 19.43%, 20.9%, 20.9% and 20.2% respectively. When polyvinyl alcohol binder is considered, 20.9%, 21.6%, 21.6% and 20.9% decomposition temperature are increased for Al₂O₃, graphene, SiC and TiO₂ nanoparticle infused Kevlar respectively. These results are presented in Fig. 8. The data indicates that addition of coating improves the decomposition temperature of Kevlar fiber. Addition of binder improves the thermal quality of the fiber. Fiber morphology effects the thermal behavior as interfere on contact area and reinforces by nanoparticles in the form of coating layer which results in more area of contact (Oyama et al., 2012). Due to this fact, improved thermal stability is obtained. Previous study shows, foam expansion is occurred in interfacial coating adjacent Kevlar surfaces due to mixing of the vinyl binders which cause better filling characteristics with acoustic thermal insulation due to char formation which is responsible for more heat protection (Pimenta et al., 2016; Nørgaard and Dam-johansen, 2012). In addition to that the coatings inclusion with vinyl resin give in higher thickness on the substrate and behave as a viscoelastic solid to liquid transaction against thermal degradation (Pimenta et al., 2016).

3.6. FTIR analysis of coated Kevlar mat

Fig. 9 represents the IR spectra of Kevlar fiber (standard) and nanoparticle deposited Kevlar fiber. The figures show that the nanoparticle deposited IR spectra has dissimilarity with the IR spectra of standard Kevlar fiber. The characteristics of bands at 2926 cm⁻¹ (C-H vibrating) of Fig. 9(b), 1504 cm⁻¹ (C=C stretching) of Fig. 9(c), 2926 cm⁻¹ (C-H vibrating) of Fig. 9(d), 1641 cm⁻¹ (C=C stretching) of Fig. 9(e), 1641 cm⁻¹ (C=C stretching) of figure-9f, 819 cm⁻¹ (Ring deformation and C-O vibrating) of Fig. 9(g), 1504 cm⁻¹ (C=C stretching) of Fig. 9h, 1506 cm⁻¹ (C=C stretching) of Fig. 9(i) were observed in the peak of nanoparticle deposited Kevlar fiber. These observations demonstrated that the nanoparticles successfully deposited on Kevlar fiber (Lee et al., 2016). The adhesion between fiber and nanoparticles are expected to increase since the fiber is now capable chemi-

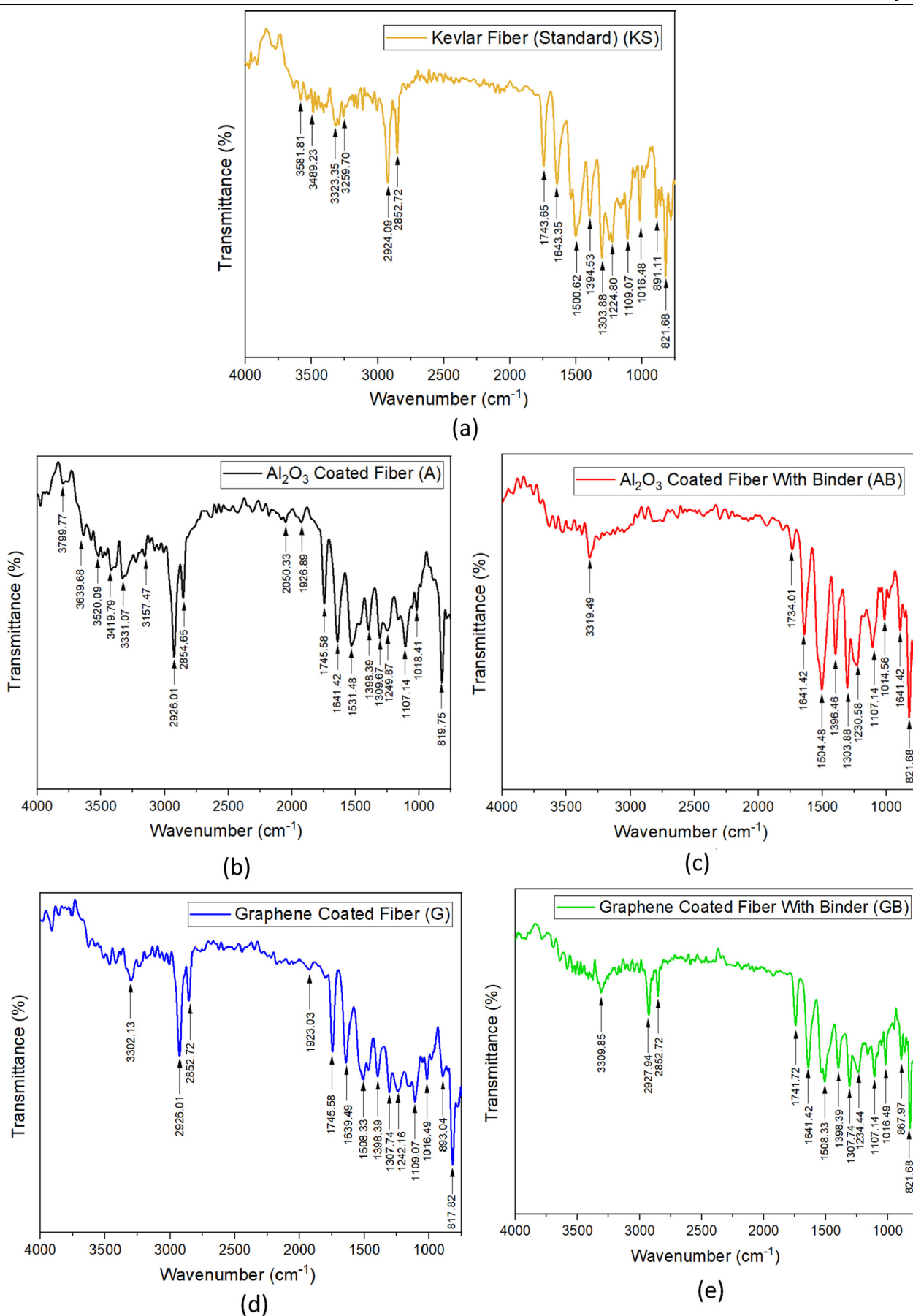


Fig. 9 ATR analysis of (a) Kevlar Fiber (Standard), (b) Al_2O_3 coated fiber, (c) Al_2O_3 coated fiber with binder, (d) Graphene coated fiber, (e) Graphene coated fiber with binder, (f) SiC coated fiber, (g) SiC coated fiber with binder, (h) TiO_2 coated fiber, (i) TiO_2 coated fiber with binder.

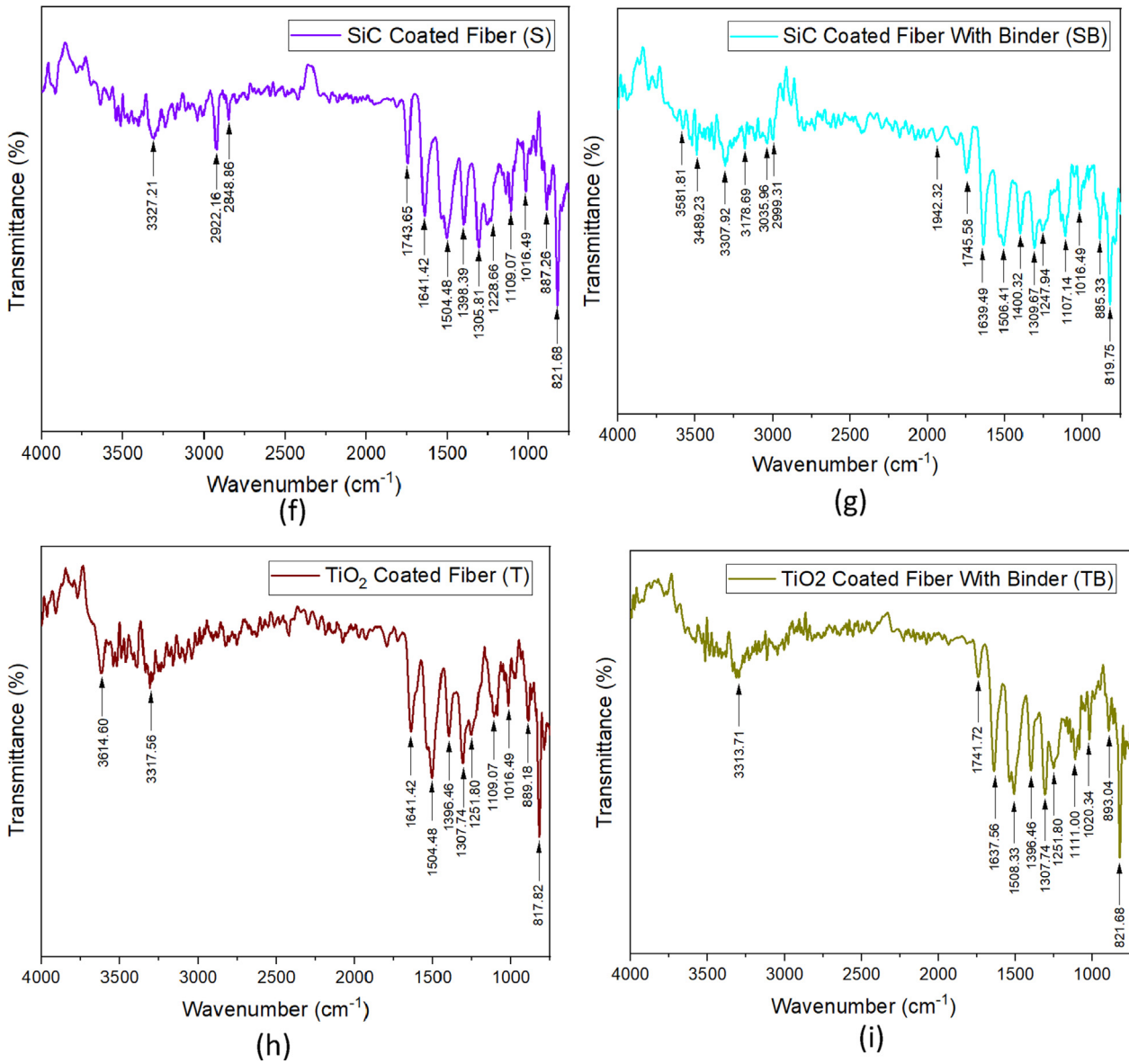


Fig. 9 (continued)

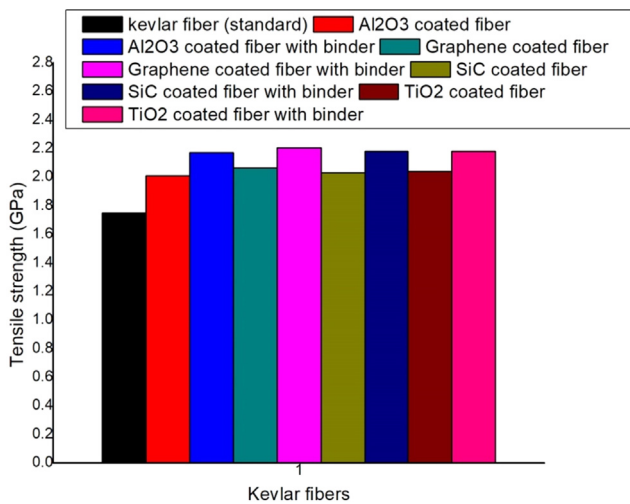


Fig. 10 Improvement of tensile strength.

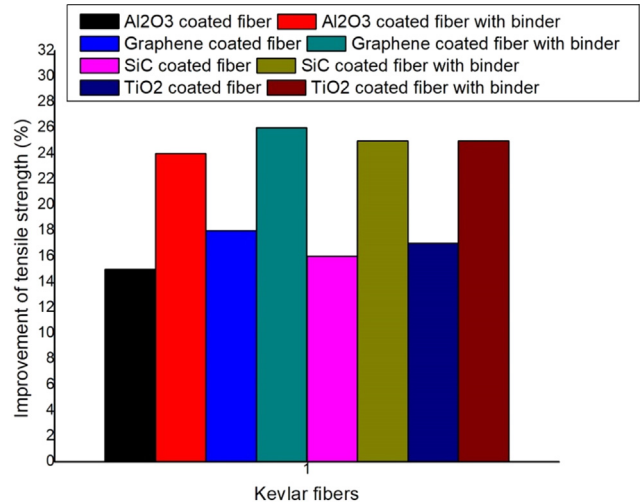


Fig. 11 Improvement of tensile strength (%).

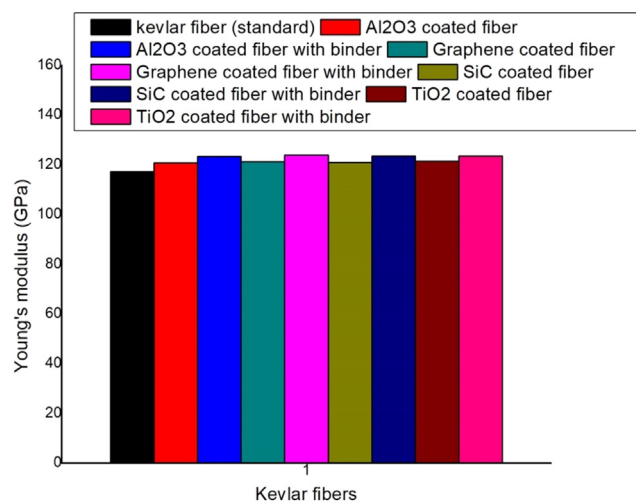


Fig. 12 Improvement of young's modulus.

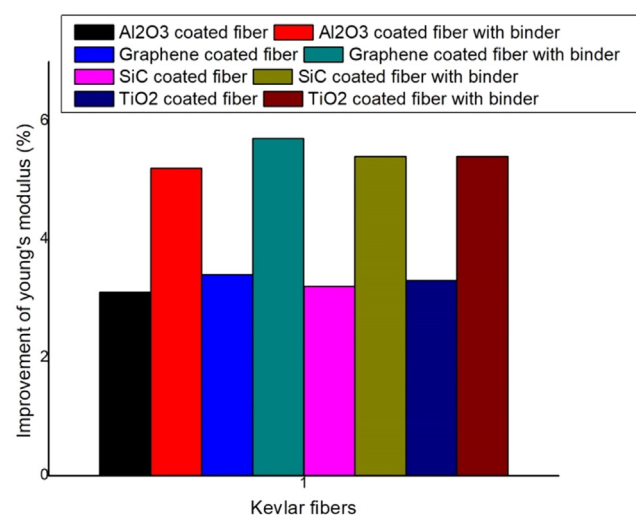


Fig. 13 Improvement of young's modulus (%).

cally to react with matrix material. The Nanoparticles are existed on Kevlar fiber is also confirmed by a SEM image. Because NPs easily form a coating layer after completing Dip-coating process.

3.7. Improvement of mechanical property of coated Kevlar mat

Fig. 10 graphically represents the improvements in tensile strength of nanoparticle coated Kevlar mat or fabric under with and without inclusion of binder. The percentage increase of tensile strength of thin film deposited kevlar mat with respect to non-coated standard Kevlar is illustrated in Fig. 11. After addition of nanoparticles as coating materials in Kevlar mat, the increase of tensile strength varies from 15% to 26%. But the percentage improvement in young's modulus varies from 3.1% to 5.7% in presence of coating nanoparticles on the surfaces of the weaving fabric. The properties of young's modulus and their percentage improvements are presented in Fig. 12 and Fig. 13. The Kevlar fibers are very

sensitive to moisture content and the limitation of Kevlar fibers is to absorb moisture quickly from the environment. The moisture content in the fibers is not only responsible to reduce their mechanical strength but also responsible for the formation of weak interfacial bonding (Isaac, 2020; Saheb and Jog, 1999). The coating on Kevlar mat prevents the moisture absorption and increase the interfacial bonding which are associated with the increase of mechanical properties. Although the fibers also exhibit high resistance against high temperature decreasing its tensile property up to 10–20% but the degradation of mechanical properties are increased further with the time (Kowsari et al., 2019). The coated Kevlar mat in this case shows better performance in relation to temperature, tensile strength and time. In general, the fibers of higher molecular weight are attributed to strong coating interlayers in relation to mechanical properties. The higher adhesion is expected because of the mechanical behaviors of the coating effect significantly the interfacial shear strength of the composite (Varelidis et al., 2000).

4. Conclusions

In this study, Nano SiC, TiO₂, Al₂O₃ and Graphene were deposited on the surface of Kevlar fiber mat via dip coating process. From this research work, it can be concluded that nanoparticles are deposited well on the surface of Kevlar fiber mats and makes interfacial adhesive bonding. The interfacial adhesion of the Kevlar mat composites can be enhanced by SiC, TiO₂, Al₂O₃ and Graphene on the surface of the Kevlar fiber mat. Dip coating process proves to be effective for the deposition of nanoparticles. Deposition of different nanoparticles improves the decomposition temperature significantly. Addition of binder adds further improvement and higher adhesion is found in NPs with binding agent due to NPs alone tend to be agglomerate because of attractive forces. Addition of graphene and graphene with binder show maximum improvement of 21.6% in decomposition temperature. Tensile strength of coated Kevlar is increased within the range of 15% to 26%. whereas young's modulus is increased within 3.1–5.7%. Stretching, vibration and decomposition of different bands confirm the successful deposition of nanoparticles on Kevlar fiber mat.

Declaration of Competing Interest

The authors declare that they have no known competing financial interests or personal relationships that could have appeared to influence the work reported in this paper.

Acknowledgement

Authors would like to acknowledge the financial support provided from Taif University Researchers Supporting Project Number (TURSP-2020/106).

References

- Anwar, Y., Ullah, I., Ul-Islam, M., Alghamdi, K.M., Khalil, A., Kamal, T., 2021. Adopting a green method for the synthesis of gold nanoparticles on cotton cloth for antimicrobial and environmental applications. *Arab. J. Chem.* 14 (9), 103327. <https://doi.org/10.1016/j.arabj.2021.103327>.
- Arriaza-Echanes, C., Campo-Giraldo, J.L., Quezada, C.P., Espinoza-González, R., Rivas-Álvarez, P., Pacheco, M., Bravo, D., Pérez-Donoso, J.M., 2021. Biomimetic synthesis of CuInS₂ nanoparticles: characterization, cytotoxicity, and application in quantum

- dots sensitized solar cells. *Arab. J. Chem.* 14 (7), 103176. <https://doi.org/10.1016/j.arabjc.2021.103176>.
- Bi, Y., Zhu, J., Xie, Z., Ren, H., 2020. Uniformly structured methyltrimethoxysilane-based silica aerogels with enhanced mechanical property by surfactant-free fabrication. *Int. J. Nanosci.* 19 (03), 1950017. <https://doi.org/10.1142/S0219581X19500170>.
- Bodke, M., Khawal, H., Gawai, U., Dole, B., 2015. Synthesis and characterization of chromium doped zinc sulfide nanoparticles. *Open Access Lib. J.* 02 (05), 1–8.
- Booker, R.D., Boysen, E., 2005. *Nanotechnology for Dummies*. John Wiley & Sons.
- Bulut, M., Alsaadi, M., Erklig, A., 2018. A comparative study on the tensile and impact properties of Kevlar, carbon, and S-glass/epoxy composites reinforced with SiC particles. *Mater. Res. Express* 5 (2), 025301. <https://doi.org/10.1088/2053-1591/aaa991>.
- Cao, K., Pons Siepermann, C., Yang, M., Waas, A.M., Kotov, N.A., Thouless, M.D., Arruda, E.M., 2013. Reactive aramid nanostructures as high-performance polymeric building blocks for advanced composites. *Adv. Funct. Mater.* 23, 2072–2080.
- Chaitep, S., Rungsiyakull, C., Watanawanyoo, P., 2009. Effects of temperature on tensile strength of Kevlar reinforced composite materials. *Int. J. Appl. Eng. Res.* 4 (10), 1979–1986.
- Chakraborty, D., Saha, S., Dey, S., Pramanik, S., 2020. Enhanced mechanical toughness of carbon nanofibrous-coated surface modified Kevlar reinforced polyurethane/epoxy matrix hybrid composites. *J. Appl. Polym. Sci.* 137 (33), 48802. <https://doi.org/10.1002/app.v137.3310.1002/app.48802>.
- Chen, Jingqin, Li, Yaoyan, Fang, Gang, Cao, Zhiyong, Shang, Yuzhi, Alfarraj, Saleh, Alharbi, Sulaiman Ali, Li, Jingjing, Yang, Siyuan, Duan, Xuelin, 2021. Green synthesis, characterization, cytotoxicity, antioxidant, and anti-human ovarian cancer activities of *Curcuma kwangsiensis* leaf aqueous extract green-synthesized gold nanoparticles. *Arab. J. Chem.* 14 (3).
- Cheng, M., Chen, W., Weerasooriya, T., 2005. Mechanical properties of Kevlar KM2 single fiber. *J. Eng. Mater. Technol.* 127, 197–203.
- Chinh, Vu Duc, Hung, Le Xuan, Palma, Luca Di, Hanh, Vu Thi Hong, Vilardi, Giorgio, 2019. Effect of carbon nanotubes and carbon nanotubes/gold nanoparticles composite on the photocatalytic activity of TiO₂ and TiO₂-SiO₂. *Chem. Eng. Technol.* 42 (2), 308–315.
- Cicco, D.e., Davide, Z.A., Taheri, F., 2017. Use of nanoparticles for enhancing the interlaminar properties of fiber-reinforced composites and adhesively bonded joints—a review. *Nanomaterials* 7 (11), 360.
- Dara, M., Hassanpour, M., Amiri, O., Baladi, M., Salavati-Niasari, M., 2021. Tb₂CoMnO₆ double perovskites nanoparticles as photocatalyst for the degradation of organic dyes: synthesis and characterization. *Arab. J. Chem.* 14 (10), 103349. <https://doi.org/10.1016/j.arabjc.2021.103349>.
- de Oliveira Braga, Fábio, Milanezi, Thiago Lara, Monteiro, Sergio Neves, Louro, Luis Henrique Leme, Vieira Gomes, Alaelson, Pereira Lima Jr., Édio, 2018. Ballistic comparison between epoxy-aramid and epoxy-aramid composites in Multilayered Armor Systems. *J. Mater. Res. Technol.* 7 (4), 541–549.
- Dorigato, A., Dzenis, Y., Pegoretti, A., 2013. Filler aggregation as a reinforcement mechanism in polymer nanocomposites. *Mech. Mater.* 61, 79–90.
- Farias, I.A.P., Santos, C.C.L., Xavier, A.L., Batista, T.M., Nascimento, Y.M., Nunes, J.M.F.F., Silva, P.M.F., Menezes-Júnior, R. A., Ferreira, J.M., Lima, E.O., Tavares, J.F., Sobral, M.V., Keyson, D., Sampaio, F.C., 2021. Synthesis, physicochemical characterization, antifungal activity and toxicological features of cerium oxide nanoparticles. *Arab. J. Chem.* 14 (1), 102888. <https://doi.org/10.1016/j.arabjc.2020.10.035>.
- Haijuan, Kong, Hui, Sun, Jin, Chai, Haiquan, Ding, Xiaoma, Ding, Muhuo, Yu, Mengmeng, Qiao, Youfeng, Zhang, 2019. Improvement of adhesion of Kevlar fabrics to epoxy by surface modification with acetic anhydride in supercritical carbon dioxide. *Polym. Compos.* 40 (S1), E920–E927.
- Ioffe, A., 2010. Kevlar fibre from DuPont. Part 2. Thermal properties and resistance to external factors. *Int. Polym. Sci. Technol.* 37 (7), 37–41.
- Isaac, Chukwuemeke William, 2020. “Crashworthiness performance of green composite energy absorbing structure with embedded sensing device providing cleaner environment for sustainable maintenance. *Sustain. Mater. Technol.* 25, e00196.
- Jana, A., Siddhalingshwar, I.G., Mitra, R., 2013. Effect of homogeneity of particle distribution on tensile crack propagation in mushy state rolled in situ Al–4.5 Cu–5TiB₂ particulate composite. *Mater. Sci. Eng., A* 575, 104–110.
- Jbara, A.S., Othaman, Z., Ati, A.A., Saeed, M.A., 2017. Characterization of γ -Al₂O₃ nanopowders synthesized by Co-precipitation method. *Mater. Chem. Phys.* 188, 24–29.
- Ke, H., Li, Y., 2018. The effects of using aluminum oxide nanoparticles as heat transfer fillers on morphology and thermal performances of form-stable phase change fibrous membranes based on capric-palmitic-stearic acid ternary eutectic/polyacrylonitrile composite. *Materials* 11 (9), 1785.
- Kowsari, Elaheh, Haddadi-Asl, Vahid, Ajdari, Farshad Boorboor, Hemmat, Jafar, 2019. Aramid fibers composites to innovative sustainable materials for biomedical applications. In: *Materials for Biomedical Engineering*. Elsevier, pp. 173–204.
- Kowsari, E., Haddadi-Asl, V., Ajdari, F.B., Hemmat, J., 2019. Aramid fibers composites to innovative sustainable materials for biomedical applications. *Mater. Biomed. Eng.*, 173–204.
- Lee, Jea Uk, Park, Byeongho, Kim, Byeong-Su, Bae, Dae-Ryung, Lee, Wonoh, 2016. Electrophoretic deposition of aramid nanofibers on carbon fibers for highly enhanced interfacial adhesion at low content. *Compos. A Appl. Sci. Manuf.* 84, 482–489.
- Li, M., Ma, W., Zhou, X., 2019. Surface modification of Kevlar fiber by nanoSiO₂ deposition in supercritical fluid. *Compos. Interfaces* 26 (10), 857–870.
- Lu, Z., Zhao, Y., Su, Z., Zhang, M., Yang, B., 2018. The effect of phosphoric acid functionalization of para-aramid fiber on the mechanical property of para-aramid sheet. *J. Eng. Fibers Fabr.* 13 (3). <https://doi.org/10.1177/155892501801300303>.
- Mahawish, A., Imad Ibrahim, S., Jawad, A.H., Mohamed Othman, F., 2017. “Effect of adding silicon carbide and titanium carbide nanoparticles on the performance of the cement pastes. *J. Civ. Environ. Eng.* 07 (04). <https://doi.org/10.4172/2165-784X10.4172/2165-784X.1000277>.
- Mahbub, R.F., Wang, L., Arnold, L., Kaneslingam, S., Padhye, R., 2014. Sinnappoo Kaneslingam, and Rajiv Padhye. Thermal comfort properties of Kevlar and Kevlar/wool fabrics. *Text. Res. J.* 84 (19), 2094–2102.
- Mekawy, M.M., Hassan, R.Y.A., Ramnani, P., Yu, X., Mulchandani, A., Xuejun, Yu, Mulchandani, Ashok, 2018. Electrochemical detection of dihydronicotinamide adenine dinucleotide using Al₂O₃-GO nanocomposite modified electrode. *Arab. J. Chem.* 11 (6), 942–949.
- Müller, K.H., Motkin, M., Philpott, A.J., Routh, A.F., Shanahan, C. M., Duer, M.J., Skepper, J.N., 2014. The effect of particle agglomeration on the formation of a surface-connected compartment induced by hydroxyapatite nanoparticles in human monocyte-derived macrophages. *Biomaterials* 35 (3), 1074–1088.
- My-Thao Nguyen, T., Anh-Thu Nguyen, T., Tuong-Van Pham, N., Ly, Q.-V., Thuy-Quynh Tran, T., Thach, T.-D., Nguyen, C.-L., Banh, K.-S., Le, V.-D., Nguyen, L.-P., Nguyen, D.-T., Dang, C.-H., Nguyen, T.-D., 2021. Biosynthesis of metallic nanoparticles from waste *Passiflora edulis* peels for their antibacterial effect and catalytic activity. *Arab. J. Chem.* 14 (4), 103096. <https://doi.org/10.1016/j.arabjc.2021.103096>.
- Nahum, T., Dodiuk, H., Kenig, S., Panwar, A., Barry, C., Mead, J., 2017. The effect of composition and thermodynamics on the

- surface morphology of durable superhydrophobic polymer coatings. *Nanotechnol. Sci. Appl.* 10, 53.
- Nazir, Arif, Akbar, Ali, Baghdadi, Hanadi B., Rehman, Shafiq ur, Al-Abbad, Eman, Fatima, Mahvish, Iqbal, Munawar, Tamam, Nissren, Alwadai, Norah, Abbas, Mazhar, 2021. Zinc oxide nanoparticles fabrication using *Eriobotrya japonica* leaves extract: photocatalytic performance and antibacterial activity evaluation. *Arab. J. Chem.* 14 (8).
- Nørgaard, K.P., Dam-johansen, K., 2012. 'Intumescent Coatings Under fast heating. *Eur. Coat. J.*, 634–639
- Oyama, H.T., Sekikawa, M., Shida, S., 2012. Effect of the interface structure on the morphology and the mechanical, thermal, and flammability properties of polypropylene/poly (phenylene ether)/magnesium hydroxide composites. *Polym. Degrad. Stab.* 97 (5), 755–765.
- Patterson, B.A., Sodano, H.A., 2016. Enhanced interfacial strength and UV shielding of aramid fiber composites through ZnO nanoparticle sizing. *ACS Appl. Mater. Interfaces* 8 (49), 33963–33971.
- Pequegnat, A., Zhou, Y., 2013. Joining of platinum (Pt) alloy wires to stainless steel wires for electronic medical devices. In: *Joining and Assembly of Medical Materials and Devices*. Woodhead Publishing, pp. 154–177.
- Pimenta, J.T., Gonçalves, C., Hiliou, L., Coelho, J.F.J., Magalhaes, F. D., 2016. Effect of binder on performance of intumescent coatings. *J. Coat. Technol. Res.* 13 (2), 227–238.
- Rajarao, R., Ferreira, R., Sadi, S.H.F., Khanna, R., Sahajwalla, V., 2014. Synthesis of silicon carbide nanoparticles by using electronic waste as a carbon source. *Mater. Lett.* 120, 65–68.
- Ren, J., Li, Q., Yan, L., Jia, L., Huang, X., Zhao, L., Ran, Q., Fu, M., 2020. Enhanced thermal conductivity of epoxy composites by introducing graphene@ boron nitride nanosheets hybrid nanoparticles. *Mater. Des.* 191, 108663. <https://doi.org/10.1016/j.matdes.2020.108663>.
- Reuben, Rachel, Joshi, Parth, Manickam, Ramachandran, 2020. Effect of copper nano powder on kevlar fiber reinforced epoxy resin composites. In: *IOP Conference Series: Materials Science and Engineering*, vol. 810, no. 1. IOP Publishing, pp. 012053.
- Saba, N., Jawaid, M., 2017. Epoxy resin based hybrid polymer composites. *Hybrid Polym. Compos. Mater.*, 57–82
- Saheb, D. Nabi, Jog, Jyoti P., 1999. Natural fiber polymer composites: a review. *Adv. Polym. Technol. J. Polym. Process. Inst.* 18 (4), 351–363.
- Sharma, S., Dhakate, S.R., Majumdar, A., Singh, B.P., 2019. Improved static and dynamic mechanical properties of multiscale bucky paper interleaved Kevlar fiber composites. *Carbon* 152, 631–642.
- Shevchenko, V.Y., Madison, A.E., 2002. Structure of nanoparticles: I. Generalized crystallography of nanoparticles and magic numbers. *Glass Phys. Chem* 28 (1), 40–43.
- Shoaib, Muhammad, Naz, Asia, Osra, Faisal Abdulrman, Abro, Shahid Hussain, Qazi, Syeda Uroos, Siddiqui, Farhan Ahmed, Raza Shah, M., Mirza, Agha Zeeshan, 2021. Green synthesis and characterization of silver-entecavir nanoparticles with stability determination. *Arab. J. Chem.* 14 (3), 102974.
- Singh, P., Shandilya, P., Raizada, P., Sudhaik, A., Rahmani-Sani, A., Hosseini-Bandegharai, A., 2020. Review on various strategies for enhancing photocatalytic activity of graphene-based nanocomposites for water purification. *Arab. J. Chem.* 13 (1), 3498–3520.
- Sreejith, M., Rajeev, R.S., 2021. Fiber reinforced composites for aerospace and sports applications. In: *Fiber Reinforced Composites*. Woodhead Publishing, pp. 821–859.
- Tian, Y., Zhang, H., Zhang, Z., 2017. Influence of nanoparticles on the interfacial properties of fiber-reinforced-epoxy composites. *Compos. A Appl. Sci. Manuf.* 98, 1–8.
- Varelidis, P.C., Papakostopoulos, D.G., Pandazis, C.I., Papaspyrides, C.D., 2000. Polyamide coated Kevlar™ fabric in epoxy resin: mechanical properties and moisture absorption studies. *Compos. A Appl. Sci. Manuf.* 31 (6), 549–558.
- Wang, Y., Chinnathambi, A., Nasif, O., Alharbi, S.A., 2021. Green synthesis and chemical characterization of a novel anti-human pancreatic cancer supplement by silver nanoparticles containing *Zingiber officinale* leaf aqueous extract. *Arab. J. Chem.* 14 (4), 103081. <https://doi.org/10.1016/j.arabjc.2021.103081>.
- Wang, S., Pei, B.o., Zhao, X., Dryfe, R.A.W., 2013. Highly porous graphene on carbon cloth as advanced electrodes for flexible all-solid-state supercapacitors. *Nano Energy* 2 (4), 530–536.
- Wen, S., Ren, H., Zhu, J., Bi, Y., Zhang, L., 2019. Fabrication of Al₂O₃ aerogel-SiO₂ fiber composite with enhanced thermal insulation and high heat resistance. *J. Porous Mater.* 26 (4), 1027–1034.
- Wen, S., Zhu, J., Yin, Q., Bi, Y., Ren, H., Zhang, L., 2020. Fabrication of infrared opacifiers loaded Al₂O₃ aerogel-SiO₂ fiber mat composites with high thermal resistance. *Int. J. Nanosci.* 19 (03), 1950021. <https://doi.org/10.1142/S0219581X19500212>.
- Xie, Zikai, Zhu, Jiayi, Bi, Yutie, Ren, Hongbo, Chen, Xuecheng, Yu, Huiyuan, 2020. Nitrogen-doped porous graphene-based aerogels toward efficient heavy metal ion adsorption and supercapacitor applications. *Physica status solidi (RRL)–Rapid Res. Lett.* 14 (1), 1900534.
- Yang, X., Tu, Q., Shen, X., Pan, M., Jiang, C., Zhu, P., Li, Y.i., Li, P., Hu, C., 2019. Surface modification of Poly (p-phenylene terephthalamide) fibers by polydopamine-polyethyleneimine/graphene oxide multilayer films to enhance interfacial adhesion with rubber matrix. *Polym. Test.* 78, 105985. <https://doi.org/10.1016/j.polymertesting.2019.105985>.
- Yang, S., Wei, B., Wang, Q.i., 2020. Superior dispersion led excellent performance of wood-plastic composites via solid-state shear milling process. *Compos. B Eng.* 200, 108347. <https://doi.org/10.1016/j.compositesb.2020.108347>.
- Yang, H.H., 1993. *Kevlar Aramid Fiber*, Chichester J. Wiley, Print.
- Zare, Y., 2016. Modeling the yield strength of polymer nanocomposites based upon nanoparticle agglomeration and polymer–filler interphase. *J. Colloid Interface Sci.* 467, 165–169.
- Zare, Y., 2016. Study of nanoparticles aggregation/agglomeration in polymer particulate nanocomposites by mechanical properties. *Compos. A Appl. Sci. Manuf.* 84, 158–164.
- Zare, Y., Garmabi, H., Sharif, F., 2011. Optimization of mechanical properties of PP/ Nanoclay/CaCO₃ ternary nanocomposite using response surface methodology. *J. Appl. Polym. Sci.* 122 (5), 3188–3200.
- Zare, Y., Garmabi, H., 2012. Nonisothermal crystallization and melting behavior of PP/nanoclay/CaCO₃ ternary nanocomposite. *J. Appl. Polym. Sci.* 124 (2), 1225–1233.
- Zeng, L., Liu, X., Chen, X., Soutis, C., 2018. Surface modification of aramid fibres with graphene oxide for interface improvement in composites. *Appl. Compos. Mater.* 25 (4), 843–852.
- Zhou, Y., Zhu, H., Zhang, W., Zuo, X., Li, Y., Yang, J., 2015. Influence of surface roughness on the friction property of textured surface. *Adv. Mech. Eng.* 7 (2). <https://doi.org/10.1177/1687814014568500>.
- Zhu, D., Mobasher, B., Rajan, S.D., 2011. Characterization of mechanical behavior of Kevlar 49 fabrics. In: Proulx, T. (Ed.), *Experimental and Applied Mechanics*, Volume 6. Conference Proceedings of the Society for Experimental Mechanics Series.